Cell Reports
Physical Science

CellPress
OPEN ACCESS

Article

Silver-free intrinsically conductive adhesives for shingled solar cells

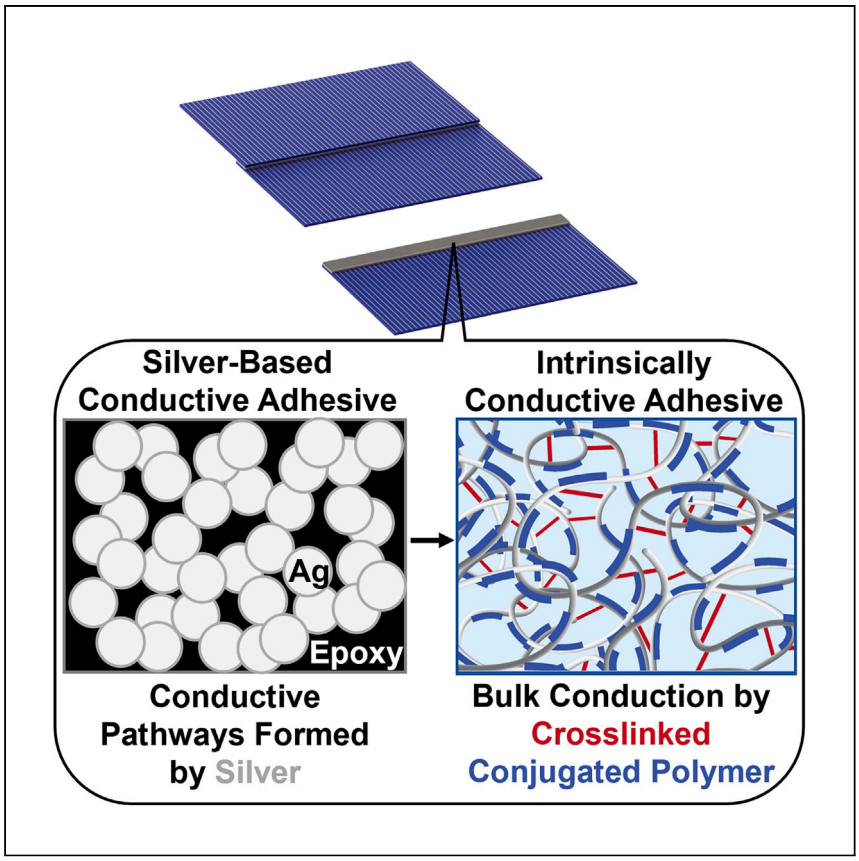

The accelerated growth of solar photovoltaics needed to reduce global carbon emissions requires an unsustainable amount of silver. Here, Chen et al. use an all-organic intrinsically conductive adhesive to replace silver-based adhesives for connecting (shingling) silicon solar cells, motivating the development of new conductive adhesive materials for sustainable, low-cost solar photovoltaics.

Alexander X. Chen, Nicholas A. Azpiroz, Sarah E. Brew, ..., Duncan W. Harwood, Darren J. Lipomi, David P. Fenning

dlipomi@ucsd.edu (D.J.L.)
dfenning@ucsd.edu (D.P.F.)

Highlights

PEDOT:PSS is used as an intrinsically conductive adhesive (ICA) to shingle solar cells

Solar cells shingled with ICAs and silver-based adhesives show comparable performances

Replacing silver-based adhesives with ICAs can significantly reduce silver consumption

Our findings motivate the design of new adhesive and conductive π-conjugated polymers

Chen et al., Cell Reports Physical Science 5, 101967
May 15, 2024
https://doi.org/10.1016/j.xcrp.2024.101967

Please cite this article in press as: Chen et al., Silver-free intrinsically conductive adhesives for shingled solar cells, Cell Reports Physical Science (2024), https://doi.org/10.1016/j.xcrp.2024.101967

Cell Reports
Physical Science

Article

Silver-free intrinsically conductive adhesives for shingled solar cells

Alexander X. Chen,[1,4] Nicholas A. Azpiroz,[2] Sarah E. Brew,[1] Antonio M. Valdez,[2] Guillermo L. Esparza,[1] Yi Qie,[1] Noah J. Valdez,[2] Rachel Blau,[1] Jordan A. Bunch,[1] Taralyn J. Perry,[2] Tarek Rafeedi,[1] Abdulhameed Abdal,[1,3] Ignasi Simon,[1] Duncan W. Harwood,[2] Darren J. Lipomi,[1,5,*] and David P. Fenning[1,6,7,*]

SUMMARY

Achieving a net-zero emissions economy by 2050 requires immediate and accelerated growth of solar photovoltaics within the next decade. However, the projected silver consumption needed for this growth is unsustainable. Here, we use poly(3,4-ethylenedioxythiophene):polystyrene sulfonate (PEDOT:PSS), a conducting conjugated polymer, as an intrinsically conductive adhesive (ICA) to replace silver-based electrically conductive adhesives (ECAs) as the adhesive interconnect for shingled solar modules. Solar cells shingled with PEDOT:PSS-based ICAs have similar photovoltaic performance metrics to those shingled with commercially available silver-based ECAs, as well as similar stability when subjected to thermal cycling. While today's dominant busbar-based modules require ~15.8 mg/W silver, we calculate that shingling modules with ICAs can reduce silver consumption to ~6.3 mg/W, accelerating our position on the silver learning curve by approximately two decades. These findings suggest that the design of π-conjugated materials for ICAs could offer a realistic strategy for sustainable deployment of lower-cost, high-power solar modules.

INTRODUCTION

The most critical materials challenge for sustainably scaling up solar photovoltaics (PVs) is currently the demand for silver.[1–3] As of 2023, the silver required for installing new solar PVs accounts for ~15–19 mg W^{-1},[4] which, at the scale of current PV production, totals ~15% of the annual supply.[5] Coupled with the growing rate of solar PV installation,[6] the Ag demand in PVs is projected to grow, as achieving the net-zero goals set out by the International Energy Agency[7] and Paris Agreement requires continued PV installation growth of 25%–30% annually for the next decade.[1,7,8] However, at the current rate of Ag consumption, solar PVs would require ~98% of the annual silver supply by 2030 (Figure S1; Table S1). While research to reduce silver consumption in solar technologies is advancing,[4] the scarcity of silver may inhibit short-term growth required by making solar modules more expensive to produce. This immediate challenge is further overshadowed by the long-term growth of solar required for this task, with extended projections suggesting a total installed capacity of ~60–75 TW needed by 2050.[1] To accelerate the transition to a decarbonized electrical grid, reducing the silver required for solar PV is a priority.

The current PV market is dominated by crystalline silicon, totaling >95% of the global market.[9,10] These silicon solar modules are made from solar cells connected

[1]Department of Nanoengineering, University of California, San Diego, 9500 Gilman Dr. Mail Code 0448, La Jolla, CA 92093, USA

[2]D2Solar, 4425 Fortran Dr. Suite F, San Jose, CA 95134, USA

[3]Department of Mechanical and Aerospace Engineering, University of California, San Diego, 9500 Gilman Dr., La Jolla, CA 92093, USA

[4]X (formerly Twitter): @alexanderxchen

[5]X (formerly Twitter): @darren_lipomi

[6]X (formerly Twitter): @dpfenning

[7]Lead contact

*Correspondence: dlipomi@ucsd.edu (D.J.L.), dfenning@ucsd.edu (D.P.F.)

https://doi.org/10.1016/j.xcrp.2024.101967

by soldered ribbons and wired together in a string.[11] This configuration poses several sources of inefficiency,[12] three of which we highlight: (1) busbars shade the frontside of the cell, (2) metal ribbons require gaps between cells, which further reduces the active area of the module, and (3) ribbons are subject to mechanical and thermal stresses that can result in substantial power losses (e.g., solder bond failure, damage to soldered joints).[13] In contrast, shingled solar modules are composed of slightly overlapping strings of solar cells that are glued together using an electrically conductive adhesive (ECA) in a manner resembling rooftop shingles.[14–16] Here, resistive losses remain along the finger length, but the areal power output is typically increased in shingled modules compared to conventional busbar designs and with better resilience to partial shading.[17] On the other hand, shingled modules can be at a cost disadvantage because more cells are used per area in a shingled module and greater loadings of silver are used per watt.

Specifically, the ECAs used for shingled modules are typically composed of conductive filler (e.g., silver particles) blended in an insulating adhesive polymer to form a paste, where 70–80 wt % of silver is required to achieve conductivities $>10^4$ S cm^{-1}.[18] The use of silver in ECA compositions poses several economic and engineering problems. First, the scarcity of silver means that the price is sensitive to supply constraints. Likewise, high loadings of electronic filler mean that the cost of the ECA, and thus the shingled module, is directly tied to the price of silver. Increasing demand for silver also poses ethical and sustainability concerns, as silver mining contributes to environmental destruction and pollution.[19,20] From an engineering standpoint, the composition of silver-based ECAs yields a trade-off between the physical properties of the polymer matrix and the electronic filler, potentially compromising either the mechanical performance of the adhesive or the electronic performance of the silver. This trade-off can be exacerbated by external (e.g., thermal) stresses due to the mechanical mismatch between the metal particles and polymer matrix. Finally, from a manufacturing standpoint, silver-based ECAs can have poor shelf lives, typically due to phase segregation (from, e.g., gravity or solvent volatility) resulting in non-uniform distribution of electronic filler and thus non-uniform conductivity and/or adhesion.

The unsustainable demand of silver creates an obstacle to the adoption of shingled architectures, as employing silver-based ECAs further exacerbates this demand. Recent research has been focused on reducing or removing silver filler in ECAs,[21] as well as the silver needed throughout the rest of the module.[4] Formulations have replaced silver with, e.g., silver-copper composites, all-copper formulations, or carbon nanotubes.[18,21] Yüce et al. developed a cost-effective formulation of silver paste with an extended shelf life by employing a capillary suspension.[22] Yu et al. fabricated high-efficiency silicon heterojunction (SHJ) solar cells with copper and tin oxide contacts.[23] Other work has explored the use of adhesive-free interconnects, particularly by busbar-busbar lamination[24] or laser welding aluminum foil between shingles.[25] Oh et al. showed that shingled solar modules could be made from cells with busbar-free electrode layouts, reducing the silver needed for metallization by ~61%.[26] Likewise, emerging research in solar cell technology has yielded busbar-less (0BB) configurations for solder-based architectures,[27] which is expected to significantly reduce silver demand. Similarly, recent advancements[28] in soldered module design have also applied gapless[29] or tiling[30] technology to reduce active area losses. Our approach replaces silver-based ECAs with a conductive polymer as the shingled interconnection, removing the need for silver filler entirely.

Please cite this article in press as: Chen et al., Silver-free intrinsically conductive adhesives for shingled solar cells, Cell Reports Physical Science (2024), https://doi.org/10.1016/j.xcrp.2024.101967

π-Conjugated (semiconducting or conducting) polymers differ from conventional polymers in chemical structure by their alternating double- and single-bond motif, which allows for charge transport. As such, conjugated polymers can be designed to behave as intrinsically plastic (e.g., stretchable and flexible) electronics.[31] However, comparatively little focus has been dedicated to designing π-conjugated polymers to function as conductive adhesives for electronic interconnects,[32] typically due to low electrical conductivities.[33] The majority of existing literature has focused on applications for biological and implantable electronics.[34,35] Among the most common π-conjugated materials is poly(3,4-ethylenedioxythiophene):polystyrene sulfonate (PEDOT:PSS), a polyelectrolyte complex with low conductivity. However, PEDOT:PSS can be doped with polar additives to significantly increase the bulk conductivity (>2,500 S cm^{-1}) of the solid film.[36,37] Likewise, recent advancements in polymer synthesis have yielded π-conjugated polymers with high intrinsic conductivities (e.g., poly(benzodifurandione), as described by the Huang[38] and Mei[39] groups).

Here, we employ PEDOT:PSS as a silver-free, intrinsically conductive adhesive (ICA) to create an interconnect between solar cells. The fundamental hypothesis is that replacing the insulating epoxy matrix of a traditional ECA with an intrinsically conductive polymer allows for the reduction or removal of silver electronic filler needed to achieve sufficient conductivity in silver-based ECAs. Even with the removal of silver filler, we achieve similar fill factors (FFs) and overall power conversion efficiency with shingled interconnects. Furthermore, employing a conducting polymer as the ICA additionally opens a myriad of opportunities for tuning the electronic, mechanical, and adhesive properties for designing next-generation electronic interconnects.

RESULTS

Formulation of silver-free conductive adhesives

In contrast to modules with soldered ribbons, shingled solar modules are glued together with an ECA, where the electronic filler is typically silver (Figure 1A).

A high loading of silver is required to form a percolated matrix throughout the adhesive and reduce the contact resistance with the substrate.[18] In contrast, the conductivity of PEDOT:PSS is dependent on the morphology of the solid film.[36,40,41] While silver-based ECAs transport charge by particle-to-particle contact or electron tunneling,[18] conductive pathways in PEDOT:PSS result from charge transport along and between polymer chains.[42] Here, we optimize ICA formulations by incorporating a silane-based crosslinker ((3-glycidyloxypropyl)trimethoxysilane [GOPS]), polar small molecules, and multi-walled carbon nanotubes (MWCNTs) into PEDOT:PSS (Heraeus, PH1000, 1.3 solid wt %) (Figure 1A; Note S1).

First, to control the dispense line of the adhesive for syringe deposition, we found an appropriate viscosity to be roughly ~10 Pa-s at 3.5 solid wt % (Figures 1B and S2). Further concentration past ~5 wt % resulted in gelling, which is possibly favorable for printing. Concentrated PEDOT:PSS was then doped with polar additives and deposited by shear deposition to investigate the electronic properties of the resulting films using 4-point probe measurements (Figures 1A, 1C, S3, and S4). While adding MWCNTs increased the conductivity of pristine PEDOT:PSS, polar dopants rendered the inclusion of electronic filler redundant. We observed that crosslinking any doped PEDOT-based film with GOPS resulted in resistivities comparable to their non-crosslinked counterparts, in agreement with our previous work.[36] Favorable PEDOT:PSS-based formulations had resistivities of $\sim 5 \times 10^{-4}$ Ω-cm, modestly higher relative to three commercial silver-based ECAs at $\sim 8 \times 10^{-5}$ Ω-cm. The conductivity of PEDOT:PSS-based films remained

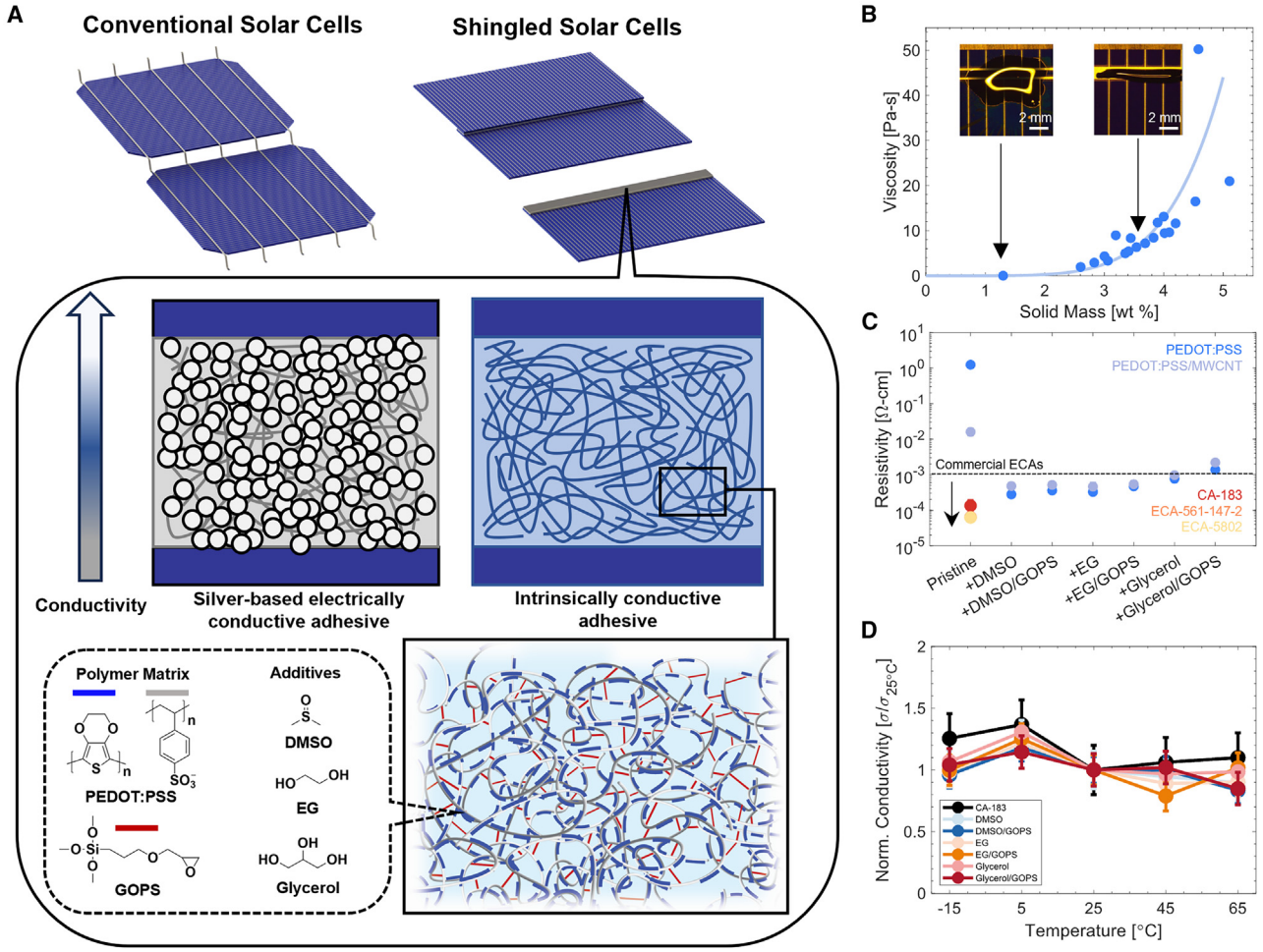

Figure 1. Design and characterization of PEDOT:PSS-based conductive adhesives

(A) Comparison of silver-based electrically conductive adhesives (ECAs) to intrinsically conductive adhesives (ICAs) for shingled solar modules. Chemical library and schematic morphology of PEDOT:PSS-based ICAs explored in this study are shown.

(B) Viscosity of PEDOT:PSS relative to solid mass in the dispersion. Inset micrographs show the dispense lines of unconcentrated PEDOT:PSS (i.e., used as received from a commercial vendor) (left) and concentrated PEDOT:PSS (right) across the busbar (2 mm scale bar width) of a silicon solar cell.

(C) Resistivity of PEDOT:PSS and PEDOT:PSS/multi-walled carbon nanotube (MWCNT) films with additives (8 vol % dimethyl sulfoxide, DMSO; 8 vol % ethylene glycol, EG; 5 vol % glycerol; 1 vol % (3-glycidoxypropyl)trimethoxysilane, GOPS). Three silver-based ECAs (red, orange, yellow) are shown for comparison. Error bars are calculated by error propagation across $n = 3$ samples.

(D) Conductivity of PEDOT:PSS and CA-183 films relative to temperature normalized to the conductivity at 25°C, with error bars calculated by error propagation across $n = 3$ samples.

relatively constant within a temperature range relevant to the typical operating conditions of solar cells (20°C–65°C)[43,44] (Figure 1D).

Shingling solar cells with silver-free conductive adhesives

Shingled cells were fabricated from Sunpreme SHJ solar cells using PEDOT:PSS-based ICAs and silver-based ECAs (Figures 2A and S5–S7). We note that all interconnected cells described here are unlaminated and unencapsulated. Lamination and encapsulation themselves can change both the mechanical and electrical properties of the adhesive joints.[24]

Cells shingled with PEDOT:PSS-based ICAs had FFs lower than but comparable to those shingled with commercial CA-183 (Figures 2B and 2C; Tables S2–S5). The

Please cite this article in press as: Chen et al., Silver-free intrinsically conductive adhesives for shingled solar cells, Cell Reports Physical Science (2024), https://doi.org/10.1016/j.xcrp.2024.101967

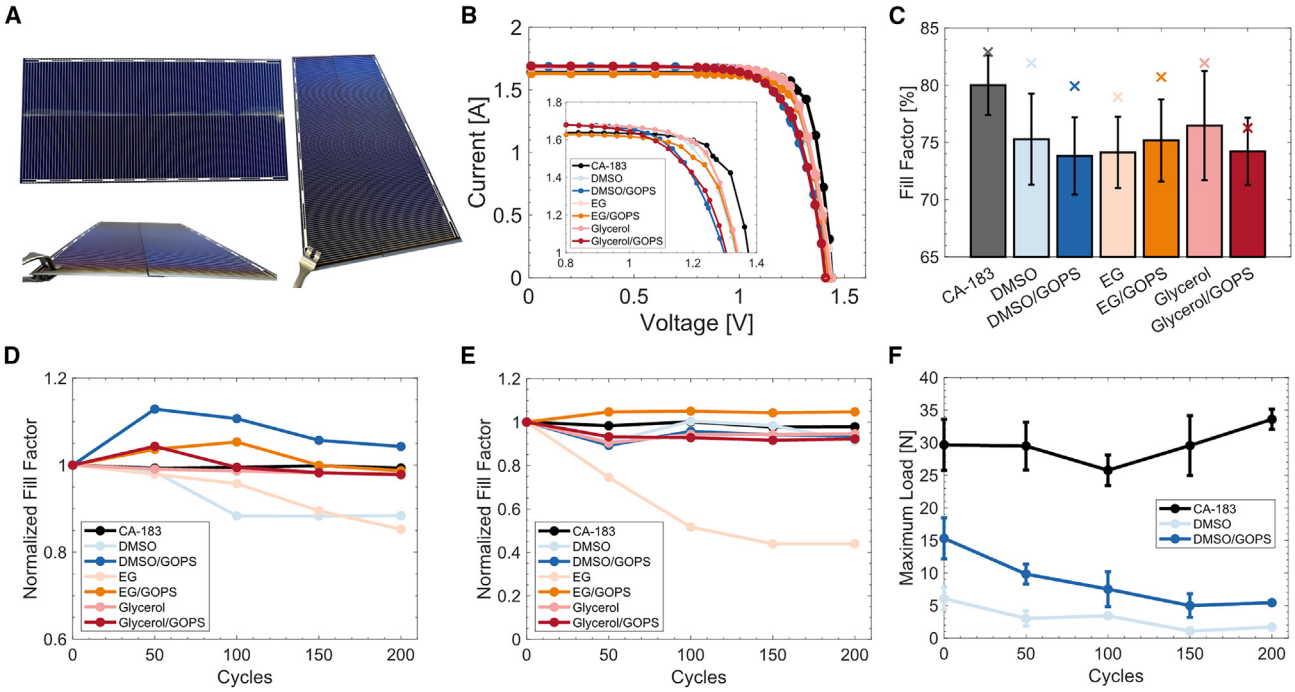

Figure 2. Characterization of shingled solar cells

(A) Photographs of interconnected silicon solar cells shingled with CA-183 (top left) and PEDOT:PSS-based (bottom left and right) ICAs.

(B) Representative current-voltage (I-V) curves of pristine interconnected cells.

(C) Fill factor of pristine cells shingled with PEDOT:PSS-based ICAs (n = 7–10) in comparison to a silver-based ECA (CA-183) (n = 13), where the "x" denotes the champion device. Error bars are reported as standard deviation.

(D) Normalized fill factor of shingled cells after being subjected to 200 thermal cycles (TC-200) from −40°C to 85°C. Three samples were individually tracked for each formulation throughout the TC-200 test, with champion samples shown here.

(E) Normalized fill factor of shingled cells after being subjected to a reverse current overload test at each 50-cycle time point. One sample was individually tracked for each formulation.

(F) Maximum load before fracture as extracted from three-point bend tests (n = 2–4) relative to thermal cycling, with error bars reported as standard deviation.

champion devices were very similar to the 83% FF of CA-183, with the glycerol-based and DMSO-based ICAs achieving ~82% FF. Because of the greater variability in the manual processing of the novel ICAs, we emphasize that these champion results exemplify what may be achievable by each ICA composition. The slightly lower champion FFs can likely be attributed to an increase in resistive losses (Figure S8), as well as the increased contact resistance for PEDOT:PSS-based ICAs ($\sim 10^{-2}$ Ω-cm^2)[36] compared to silver-based ECAs ($\sim 10^{-3}$ Ω-cm^2). Likewise, crosslinked PEDOT:PSS formulations typically showed slightly lower FFs than their non-crosslinked counterparts, which can again possibly be explained by a further increase in contact resistance ($\sim 10^{-1}$ Ω-cm^2).[36] Nevertheless, champion crosslinked ICAs incorporating DMSO/GOPS and EG/GOPS achieve >80% FF in these preliminary experiments. Overall, across the various formulations tested, the average FF of ICA-shingled cells was slightly lower than CA-183 (~5%). The reasonably close performance of these proof-of-principle ICAs to CA-183 is put into context considering that PEDOT:PSS is not optimized for such application, as well as the absence of years of process engineering conducted for optimizing the fabrication process relative to the commercial ECA.

Accelerated degradation of silver-free conductive adhesives

Given the competitive performance of the ICAs, we moved to examine the durability of the ICAs relative to commercial ECAs in accelerated stress tests of the material

and in shingled cell formats. In damp heat testing at 65°C and 65% relative humidity (RH; ISOS-D-3, as is used for emerging solar cell technologies[45]), the introduction of crosslinking by the addition of GOPS reduced, but did not fully mitigate, the impact of moisture ingress on both the electrical conductivity and microstructure (e.g., swelling, delamination, and moisture-driven decohesion[46]) (Figures S4 and S9–S17). The degradation induced by heat and moisture is attributed to morphological rearrangement within the PEDOT:PSS film, in good agreement with prior literature.[47–49] Given that heating at ambient humidity did not strongly affect conductivity (Figure 1D) at typical operating temperatures for solar cells (15°C–65°C), electrical degradation in PEDOT:PSS films appears to be primarily moisture driven. PEDOT:PSS-based ICAs would likely benefit from edge-sealed, glass-glass PV packages that are used for thin-film PVs and are increasingly common for bifacial silicon modules, in which exposure to moisture is excluded.[50,51] More detailed discussion on moisture-induced degradation mechanisms at elevated temperature and RH is included in the supplemental information (Note S2).[46–49,52]

We subjected cells interconnected with ICA formulations and control ECAs to accelerated degradation tests by thermal cycling from 85°C to −40°C following the IEC standard test (Figures 2D and S18).[53] While thermal cycle tests are typically performed on encapsulated strings, this initial durability test was used to investigate the effect of temperature cycling on the adhesive itself. Encouragingly, all crosslinked ICAs showed comparable performance to CA-183 in terms of relative FF, albeit with more variability in PV performance (Table S2). In contrast, PEDOT:PSS/EG and PEDOT:PSS/DMSO showed significant degradation after 50 cycles. These data suggest that crosslinking preserves the electronically favorable morphology, with electronic degradation for non-crosslinked ICAs attributed to morphological rearrangement. Interestingly, PEDOT:PSS/glycerol showed comparable performance to crosslinked ICAs while also having an increased FF (Figure S18). This stability can possibly be attributed to residual glycerol remaining in the film due to its high boiling point (290°C, compared to 189°C for DMSO and 197°C for EG), preserving the favorable electronic morphology induced by secondary doping at relevant temperatures.

Electrical degradation was then incorporated into thermal aging tests by subjecting shingled cells to reverse current overload (RCO) tests (Figures 2E; Table S6). Most PEDOT:PSS-based ICAs still showed comparable stability under RCO loads to commercial CA-183, with slightly greater degradation but remaining within 10% of their original FFs. Strikingly, PEDOT:PSS/EG/GOPS outperformed CA-183. The accelerated degradation observed was especially transparent for PEDOT:PSS/EG, which showed a ∼15% relative decrease in FF from thermal cycling but a ∼55% decrease when RCO was incorporated.

Finally, three-point bend (3PB) tests were performed on shingled cells that were subjected to temperature cycling (Figures 2F and S19). We hypothesized that thermal stresses would weaken the adhesion of PEDOT:PSS-based ICAs due to temperature-driven rearrangement of the film morphology and that this morphological reorganization[47] could be impeded by crosslinking. Typically, crosslinked ICAs withstood greater loads than their non-crosslinked counterparts, suggesting some adhesive benefit to crosslinking. However, both non-crosslinked and crosslinked ICAs generally showed a decrease in maximum load relative to increased thermal degradation, while CA-183 remained relatively stable. Most striking was the difference in failure mechanisms. While cells shingled with CA-183 failed cohesively (within a silicon cell), cells shingled with PEDOT:PSS-based ICAs failed adhesively (within the adhesive lap joint) (Figure S19). The failure modes observed from 3PB

Please cite this article in press as: Chen et al., Silver-free intrinsically conductive adhesives for shingled solar cells, Cell Reports Physical Science (2024), https://doi.org/10.1016/j.xcrp.2024.101967

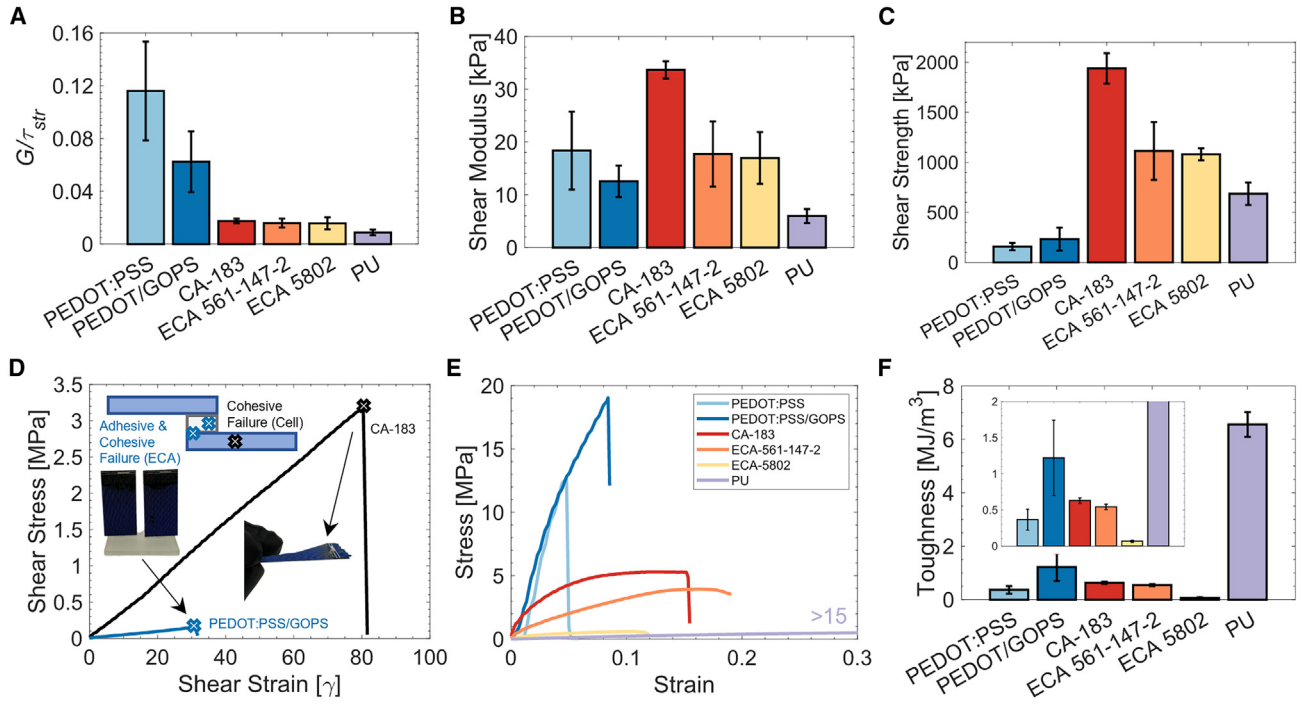

Figure 3. Mechanical properties of PEDOT:PSS-based and silver-based conductive adhesives

(A–C) Figure of merit for shingled interconnections (A): ratio of shear modulus (B) to shear strength (C) as calculated from the respective parameters extracted from lap shear tests.

(D) Stress-strain curves of lap shear tests performed with silicon solar cell substrates.

(E) Stress-strain curves of ECAs investigated in this study as measured using tensile tests.

(F) Toughness of ECAs investigated in this study as extracted from stress-strain curves.

All error bars are reported as standard deviation with at least $n = 3$ samples.

tests suggest that the primary weakness of PEDOT:PSS-based ICAs is the adhesive functionality.

Comparing the mechanical performance of conductive adhesives

To understand the differences in mechanical performance between PEDOT:PSS-based and silver-based conductive adhesives, we performed lap shear and tensile tests (Figure 3). Beaucarne previously suggested that the ratio of shear modulus to adhesive strength ($G\ \tau_{str}^{-1}$) is an important figure of merit (FOM) for shingled interconnections.[12] To reduce the likelihood of mechanical failure, the shear modulus should be minimized and adhesive strength maximized (Figure 3A). The $G\ \tau_{str}^{-1}$ values extracted from lap shear tests differed significantly from ideal parameters,[12] stemming from an overestimation of the shear strain due to the testing method (Figure S20; Table S7). However, qualitative trends showed that PEDOT:PSS had the highest $G\ \tau_{str}^{-1}$ values, roughly one magnitude greater than silver-based ECAs. Crosslinking offered a modest reduction in $G\ \tau_{str}^{-1}$, but these FOMs were still not comparable to silver-based ECAs.

As a comparison for what is achievable using polymeric materials, a commercial polyurethane (PU) (which had the lowest calculated $G\ \tau_{str}^{-1}$) was included as a reference. The primary differences in $G\ \tau_{str}^{-1}$ values were due to the adhesive strengths, which differed significantly in comparison to the shear moduli (Figures 3B and 3C). This difference is relatively unsurprising, as PEDOT:PSS is used here as an ersatz adhesive. Crosslinking with GOPS increased the cohesive strength by creating a

crosslinked network between PSS chains, but poor adhesion at the interface remained an avenue for delamination. These differences in failure mechanisms were stark when shear tests were performed using silicon cells as substrates. Similarly to 3PB tests, the fracture of the module occurred cohesively for CA-183, while PEDOT:PSS/GOPS experienced mixed failure, suggesting debonding occurring both at the PEDOT:PSS/silicon interface and within the adhesive joint (Figure 3D).

Tensile tests were performed to compare cohesive behavior and thus elucidate differences in energy dissipation (Figures 3E and S21; Table S8). PEDOT:PSS and PEDOT:PSS/GOPS were brittle with high tensile strengths, suggesting little flow of the polymer chains and few energy dissipation mechanisms by plastic rearrangement. However, PEDOT:PSS/GOPS had a greater toughness than all silver-based ECAs measured (Figure 3F). Similarly, PU showed the greatest toughness of all materials yet a lower adhesive strength than all silver-based ECAs. These observations suggest that the primary contribution to the high adhesive strength of the silver-based ECAs is the energy dissipation at the interface (substrate/adhesive) rather than the dissipation within the bulk material. Given the relevant electronic performance and early durability results of the ICAs, future work to increase the adhesion of the ICA could benefit from using the many levers of polymer design (e.g., synthetic modification, addition of tackifiers or crosslinkers, polymer blending). Increasing the adhesion of ICAs while maintaining the favorable electronic performance may enable drop-in replacements for silver-based commercial conductive adhesives.

Implications of silver-free ICAs for PV scaling

We examine the broader impacts of removing silver from the adhesive interconnect for shingled solar modules on the consumption of silver by solar PVs (Figure 4).

The two primary advantages of replacing silver-based ECAs with all-organic ICAs are related to the scarcity and price variability of silver. High filler loadings mean that the price of silver-based ECAs is tied directly to silver, which has fluctuated between \$300 and \$1,500 kg^{-1} since 2006.[54] In contrast, polymeric materials can be manufactured synthetically at large scales and thus are far cheaper due to economies of scale.[55] As such, the current price of PEDOT:PSS is one-third that of silver, despite far fewer industrial applications (Figure 4A). The annual supply of silver has remained relatively constant (~29 kt $year^{-1}$), while the demand for silver for solar PVs has been steadily increasing (Figures 4B and S1). This trend suggests that a significantly increased demand for silver could result in increases in the cost of silver.

To compare the silver required for scaling up solar PVs, we calculate projections of silver consumption as demanded by busbar architectures and shingled architectures (with silver-based or silver-free ECAs) (Figure 4C; Table S9–S11). For soldered-ribbon modules and modules shingled with silver-based ECAs, the silver needed to fulfill a 75 TW transition to solar PVs by 2050 is unsustainable. Optimistic calculations suggest that busbar modules would essentially consume the entire silver reserve, while the silver required for conventionally shingled modules far exceeds global supply. Recycling silver from PV modules is an option but remains a challenge, as the current supply of end-of-life modules does not make it economically viable to scale up recycling efforts.[56,57] We note that our estimations approximate that ~13 mg/W silver is required per ECA-shingled joint for PERC cells. Work by Tune et al. suggests there are scenarios in which this is an overestimate, predicting about ~5 mg/W silver will be required for shingled modules[58] when accounting for projected advancements in ECA technologies with reduced silver content. This range is captured with the lower bound of our estimation cone (5.19 mg/W).

Please cite this article in press as: Chen et al., Silver-free intrinsically conductive adhesives for shingled solar cells, Cell Reports Physical Science (2024), https://doi.org/10.1016/j.xcrp.2024.101967

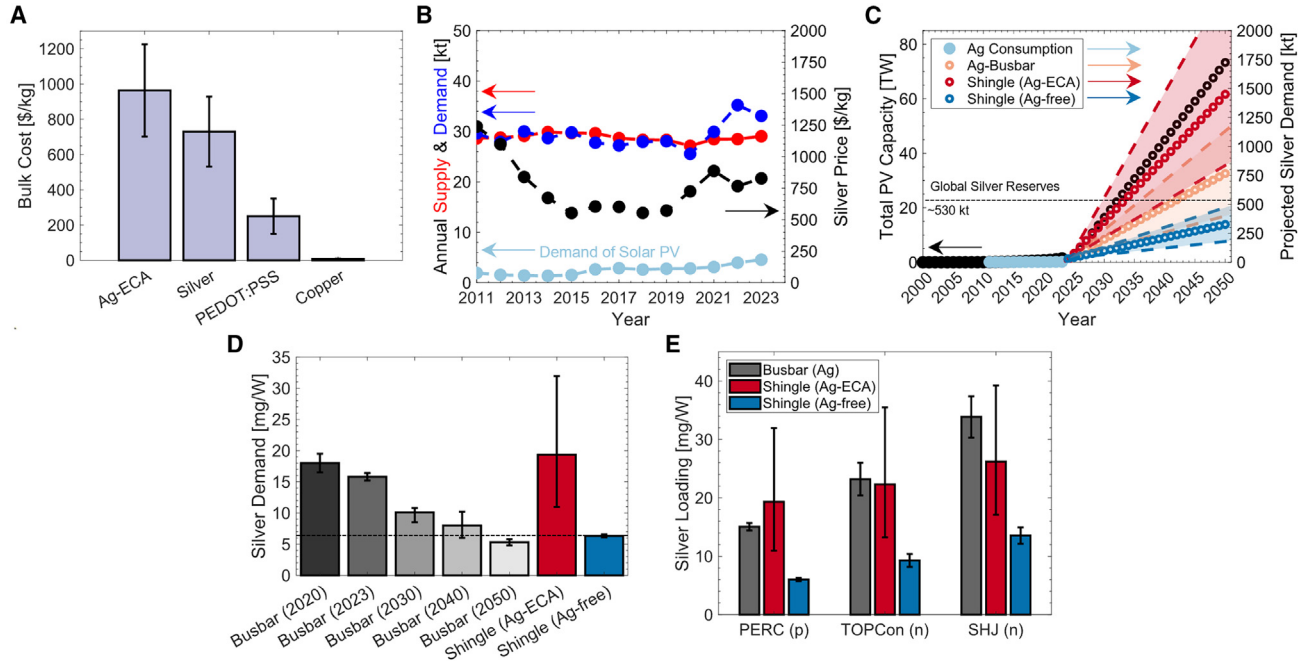

Figure 4. What is the impact of reducing silver in shingled solar modules?

(A) Comparison of bulk cost of common interconnect materials. Average prices for silver and copper were reported as the spot price of each metal in August 2023, with the error reported as the peak and valley prices during 2023. As the price of silver-based ECAs is strongly tied to the price of silver itself,[54] the average price and error reported are estimated using a 30% markup. The price of PEDOT:PSS was reported as the bulk price as quoted by Heraeus. The error was estimated by collecting several quotes for 1 kg PEDOT:PSS and determining the peak and valley prices (as a percentage of the mean price).

(B) Annual supply and demand of silver relative to the demand of silver from solar PVs and price.

(C) Projected demand of silver relative to total PV capacity installed for busbar and shingled modules (both silver based and silver free). Red, orange, and blue circles represent median estimations, with dashed lines representing high and low projections. Marked is the total global silver reserve.

(D) Comparison of silver consumption for busbar and shingled modules.

(E) Comparison of current silver consumption for silicon cell architectures (passivated emitter and rear contact, PERC); tunnel oxide passivated contact, TOPCon; and silicon heterojunction, SHJ) using busbar and shingled interconnects.

Detailed descriptions of how error was calculated for each analysis are included in the supplemental information (Note S3).

Using silver-free ECAs (e.g., ICAs) for shingled modules significantly reduces the amount of silver required. From work by Oh et al., we assumed that shingling cells would allow for a 60% decrease in silver required for metallization in comparison to conventional modules due to the removal of the busbars.[26] With a current silver consumption of ~15.8 mg W^{-1}, this approximation suggests that only ~6.3 mg W^{-1} is required for current (p-type PERC) shingled modules using silver-free ECAs (Figure 4D). Assuming that projections for the silver learning curve[4] directly apply, we find that an immediate (but unrealistic) transition to modules shingled with silver-free ECAs prevents silver usage from exceeding global supply (Figure 4C). Calculations by Hallam et al. suggest that a silver consumption of ~5 mg W^{-1} is achievable with progression along the learning curve by 2050.[4] As such, a reduced consumption rate of ~6.3 mg W^{-1} for modules shingled with silver-free ECAs immediately accelerates our placement on the learning curve to >2040 (Figure 4D). Thus, development of silver-free ECAs offers an avenue for reducing the silver usage of solar PVs. We note that this analysis conducted for ICA-shingled modules is similar to what could be achieved for an immediate, though unrealistic, transition to solder-based 0BB designs[59] if solder wires to fingers in 0BB technology are silver-free and a similar silver-loading and shaded area in the front-side fingers were achieved. Likewise, we note that the estimation of silver

Please cite this article in press as: Chen et al., Silver-free intrinsically conductive adhesives for shingled solar cells, Cell Reports Physical Science (2024), https://doi.org/10.1016/j.xcrp.2024.101967

consumption for soldered-ribbon modules accounts for advancements in solar module design through the range of low and high projections. Finally, our calculations suggest that a switch from busbar modules to shingled modules could possibly accelerate the transition from p-type PERC (which currently dominates the PV market[8]) to high-efficiency n-type (particularly TOPCon and SHJ) cells due to the reduction in silver needed for metallization (Figures 4E and S22).

DISCUSSION

In this study, we employed PEDOT:PSS as an ICA for shingling solar cells for high-efficiency shingled modules. Doping concentrated solutions of PEDOT:PSS with DMSO, EG, or glycerol increased the electrical conductivity, removing the need for any Ag filler. To stabilize the morphology and increase the cohesive strength, we formed a crosslinked PSS network within the deposited adhesive using GOPS. Solar cells shingled with PEDOT:PSS-based ICAs had the same open-circuit voltage (V_{oc}) and short-circuit current (I_{sc}), and achieved champion FFs of ~82%, only ~1% absolute lower than cells interconnected with silver-based ECAs. Crosslinking proved to be effective in preserving the favorable electronic morphology against thermal cycling, with crosslinked ICAs showing comparable stability to commercial silver-based ECAs. Interestingly, PEDOT:PSS/glycerol also showed comparable stability, likely due to residual dopant remaining in the adhesive due to the high boiling point of glycerol. Critically, replacing silver-based ECAs with ICAs significantly reduces the silver demanded by the solar module.

The results indicate a new application for conjugated polymers for solar PVs and motivate the rational design of ICAs. The primary weakness of PEDOT:PSS-based ICAs here was the poor adhesive functionality. Simple approaches for improving both the adhesive and cohesive behavior could involve blending with adhesive polymers (e.g., epoxies, PUs). We expect future work to take advantage of the incredible diversity of conjugated polymers and synthetic avenues to replace PEDOT:PSS with purpose-made polymers with both high intrinsic conductivities[38,39] and excellent adhesive functionality. Such challenges are addressable by synthetic methods and rational design for (1) tuning the mechanical and electronic properties of conjugated polymers[34,60–63] and (2) tuning the adhesive properties of non-conjugated polymers.[64,65] As such, this approach offers a realistic avenue toward reducing the amount of silver required to scale up solar PVs as needed to sustainably decarbonize the electrical grid.

EXPERIMENTAL PROCEDURES

Resource availability

Lead contact

Requests for further information should be directed to the lead contact of this study, David P. Fenning (dfenning@ucsd.edu).

Materials availability

No new materials were generated for this study.

Data and code availability

Detailed descriptions and methodology describing calculations performed and data generated during this study are available in the main text and supplemental information.

Material selection

The primary goal of this work is to use a conducting polymer matrix as an adhesive interconnect for shingled solar cells in order to reduce the use of silver as an

Please cite this article in press as: Chen et al., Silver-free intrinsically conductive adhesives for shingled solar cells, Cell Reports Physical Science (2024), https://doi.org/10.1016/j.xcrp.2024.101967

electronic filler. We elected to use a commercially available formulation of PEDOT:PSS (Clevios PH1000, Heraeus) because metal-free (secondary) doping methods are well studied in literature, despite PH1000 not being designed for use as a conductive adhesive, and the materials are widely available. To control the adhesive dispense line of PEDOT:PSS, we increased the viscosity by removing water from the dispersion using a rotary evaporator. Here, we elect to use polar small molecules (DMSO, EG, glycerol) as secondary dopants for increasing the bulk conductivity without inclusion of metal filler. Preliminary design-of-experiment investigations suggested that the ideal loadings of DMSO, EG, and glycerol were 8, 8, and 5 vol %, respectively. In order to increase the cohesive strength of the PEDOT:PSS film, we form a crosslinked matrix within the PEDOT:PSS film using a silane crosslinker (GOPS, 1 vol %). In addition to improving the mechanical robustness, GOPS is also used to stabilize the PEDOT:PSS film (i.e., under continuous thermal or electrical cycling) and reduce moisture ingress (e.g., swelling). To improve the dispensability of the material and reduce spreading (for a consistent adhesive dispense line) before use, water was removed from PEDOT:PSS using a rotary evaporator to achieve viscosities of ~10 Pa-s. We also explored the use of a custom-synthesized PEDOT:PSS copolymer (PEDOT:PSS_1-*b*-$PPEGMEA_6$) for the adhesive matrix because we hypothesized that the soft, stretchable PPEGMEA block would increase the viscoelastic adhesion of the material (Note S1).[66] However, we found that Block-6 showed significantly higher resistivities compared to PEDOT:PSS when blended with polar additives and cast in a solid film, suggesting weaker secondary doping effects (Note S1; Figure S23).

Electronic and mechanical characterization

Shingled solar cells were formed by gluing together Sunpreme 4-busbar silicon cells using different formulations of PEDOT:PSS. These formulations were compared to different commercially available formulations of silver-based ECAs. Shingled cells were subjected to thermal aging by temperature cycling from −40°C to 85°C as an accelerated degradation test. At 50-cycle intervals throughout the degradation test, the performance of shingled cells was characterized using I-V measurements, RCO tests, and 3PB tests. For RCO tests, samples were subjected to a constant current of 4, 6, 8, and 10 A for 120 s, with an I-V curve taken immediately after each step. To isolate the effect of the ICA composition on the resistive losses, the series resistance was extracted from each I-V curve using a standard single-diode model. Further information describing solar cell characterization is available in the standard data reporting for PV cells (Data S1). To further characterize the mechanical behavior of PEDOT:PSS as an adhesive lap joint (particularly in comparison to commercial ECAs), we performed tensile tests and lap joint shear tests. Finally, to further understand the degradation behavior of PEDOT:PSS, degradation tests were performed on blade-coated films (to mimic common shear deposition techniques used to deposit polymer films for commercial processes). These PEDOT:PSS films were subjected to 65% RH at 25°C, 65% RH at 65°C, and 100% RH (a water bath) at 65°C. Detailed descriptions of the above methods are described in the supplemental experimental procedures.

Economic analysis

Data for the economic analyses performed in this study were gathered from publicly available databases and existing literature. Data on the supply, demand, and price of silver were obtained from annual World Silver Survey reports published by the Silver Institute.[5] Data on installed solar PV capacity were obtained from Our World in Data.[6] Projections for total installed solar capacity assumed a total installation of 341.5 GW in 2023,[5] a 30% growth in total capacity until 2030, and finally steady-state growth from 2030 to 2050 (Table S1). Data used for projections of silver demand

until 2050 were obtained from reports published by the International Energy Agency,[7] the International Technology Roadmap for Photovoltaic,[8] and work by Hallam et al.[3,4] Data on the pricing of PEDOT:PSS were obtained from Heraeus, and the standard error was calculated from the price variation for PEDOT:PSS (with an approximately equivalent solid mass concentration, ~1.3 wt %) from several vendors. In order to estimate the demand and cost of silver used for shingled solar modules, approximations were made regarding the ECA/ICA thickness and adhesive overlap,[67] silver consumption for busbar-free modules,[26] silver loading and price of conductive adhesives,[54] and total required solar PV capacity installed by 2050.[1] Detailed descriptions of the calculations performed are described in the supplemental information.

SUPPLEMENTAL INFORMATION

Supplemental information can be found online at https://doi.org/10.1016/j.xcrp.2024.101967.

ACKNOWLEDGMENTS

This work was supported by the Air Force Office of Scientific Research (AFOSR) grant no. FA9550-22-1-0454 to D.J.L. and by the California Energy Commission (CEC) grant no. EPC-19-004 to D.P.F. A.X.C. acknowledges support from the UC President's Dissertation Year Fellowship. R.B. acknowledges financial support from the European Union's Horizon 2020 Research and Innovation Programme under the Marie Skłodowska-Curie grant agreement no. 898571. A.A. acknowledges support from the Kuwait Foundation for the Advancement of Sciences (KFAS). This work was performed in part at the San Diego Nanotechnology Infrastructure (SDNI) of UC San Diego, a member of the National Nanotechnology Coordinated Infrastructure, which is supported by the National Science Foundation (grant ECCS-2025752). The authors would like to thank Andrew Hu for his support and helpful discussions.

AUTHOR CONTRIBUTIONS

A.X.C., D.J.L., and D.P.F. conceptualized the project. A.X.C. and D.P.F. designed the experiments. A.X.C., N.A.A., A.M.V., S.E.B., N.J.V., Y.Q., G.L.E., J.A.B., T.J.P., I.S., and D.W.H. conducted experiments and were responsible for data collection. Y.Q. and R.B. provided the custom-synthesized material (Block-6) used in this study. A.X.C., N.A.A., G.L.E., and D.W.H. were responsible for calculations and data analysis. A.X.C. was responsible for data visualization. A.X.C., T.R., and A.A. made the figures. A.X.C., D.W.H., and D.P.F. were responsible for project supervision. A.X.C. and D.P.F. were responsible for project management and administration. D.W.H., D.J.L., and D.P.F. were responsible for funding acquisition. D.W.H., D.J.L., and D.P.F. provided the equipment and resources used in this study. A.X.C. wrote the original draft of the manuscript. A.X.C., D.J.L., and D.P.F. reviewed and edited the manuscript. All authors reviewed and provided feedback on the manuscript before submission.

DECLARATION OF INTERESTS

The authors have filed a provisional patent describing the use of silver-free ICAs for shingling solar cells (No. 63/556,356).

Received: October 15, 2023
Revised: March 18, 2024
Accepted: April 16, 2024
Published: May 6, 2024

REFERENCES

1. Haegel, N.M., Verlinden, P., Victoria, M., Altermatt, P., Atwater, H., Barnes, T., Breyer, C., Case, C., De Wolf, S., Deline, C., et al. (2023). Photovoltaics at multi-terawatt scale: Waiting is not an option. Science *380*, 39–42. https://doi.org/10.1126/science.adf6957.

2. Goe, M., and Gaustad, G. (2014). Identifying critical materials for photovoltaics in the US: A multi-metric approach. Appl. Energy *123*, 387–396. https://doi.org/10.1016/j.apenergy.2014.01.025.

3. Zhang, Y., Kim, M., Wang, L., Verlinden, P., and Hallam, B. (2021). Design considerations for multi-terawatt scale manufacturing of existing and future photovoltaic technologies: Challenges and opportunities related to silver, indium and bismuth consumption. Energy Environ. Sci. *14*, 5587–5610. https://doi.org/10.1039/d1ee01814k.

4. Hallam, B., Kim, M., Zhang, Y., Wang, L., Lennon, A., Verlinden, P., Altermatt, P.P., and Dias, P.R. (2022). The silver learning curve for photovoltaics and projected silver demand for net-zero emissions by 2050. Progress in Photovoltaics. *31*, 598–606. https://doi.org/10.1002/pip.3661.

5. Newman, P., Meader, N., Klapwijk, P., Chou, E., Gao, Y., Barot, H., Yau, S., Liang, J., Rey, F., Smith, J., et al. (2023). World Silver Survey 2023.

6. Installed Solar Energy Capacity (2023). Our World Data.

7. International Energy Agency (2021). Net Zero by 2050: A Roadmap for the Global Energy Sector.

8. Fischer, M., Woodhouse, M., Baliozian, P., and Trube, J. (2023). International Technology Roadmap for Photovoltaic.

9. Battaglia, C., Cuevas, A., and De Wolf, S. (2016). High-efficiency crystalline silicon solar cells: Status and perspectives. Energy Environ. Sci. *9*, 1552–1576. https://doi.org/10.1039/c5ee03380b.

10. Masson, G., and Kaizuka, I. (2022). Photovoltaic Power Systems Programme Annual Report 2022.

11. Beaucarne, G., Schubert, G., Tour, L., and Hoornstra, J. (2019). Summary of the 8th Workshop on Metallization and Interconnection for Crystalline Silicon Solar Cells. AIP Conf. Proc. 020001, 1–13.

12. Beaucarne, G. (2016). Materials challenge for shingled cells interconnection. Energy Proc. *98*, 115–124.

13. Asadpour, R., Sulas-Kern, D.B., Johnston, S., Meydbray, J., and Alam, M.A. (2020). Dark lock-in thermography identifies solder bond failure as the root cause of series resistance increase in fielded solar modules. IEEE J. Photovoltaics *10*, 1409–1416. https://doi.org/10.1109/JPHOTOV.2020.3003781.

14. Schmidt, W., and Rasch, K.D. (1990). New Interconnection Technology for Enhanced Module Efficiency. IEEE Trans. Electron. Dev. *37*, 355–357. https://doi.org/10.1109/16.46366.

15. Werner, J., Boyd, C.C., Moot, T., Wolf, E.J., France, R.M., Johnson, S.A., Van Hest, M.F.A.M., Luther, J.M., Zhu, K., Berry, J.J., and McGehee, M.D. (2020). Learning from existing photovoltaic technologies to identify alternative perovskite module designs. Energy Environ. Sci. *13*, 3393–3403. https://doi.org/10.1039/d0ee01923b.

16. Shepard, N.F. (1979). Development and Testing of Shingle-Type Solar Cell Modules. https://doi.org/10.2172/5868348.

17. Kunz, O., Evans, R.J., Juhl, M.K., and Trupke, T. (2020). Understanding partial shading effects in shingled PV modules. Sol. Energy *202*, 420–428. https://doi.org/10.1016/j.solener.2020.03.032.

18. Aradhana, R., Mohanty, S., and Nayak, S.K. (2020). A review on epoxy-based electrically conductive adhesives. Int. J. Adhesion Adhes. *99*, 102596. https://doi.org/10.1016/j.ijadhadh.2020.102596.

19. Artiola, J.F., Walworth, J.L., Musil, S.A., and Crimmins, M.A. (2019). Soil and Land Pollution, 3rd ed. (Elsevier Inc.). https://doi.org/10.1016/b978-0-12-814719-1.00014-8.

20. Kim, T.-Y., Gould, T., Bennett, S., Boutin, H., Buisson, E., Dasgupta, A., Deguchi, T., Gouy, A., Kim, Y.Y., Michaels, K.C., et al. (2023). Critical Minerals Market Review 2023.

21. Zemen, Y., Schulz, S.C., Trommler, H., Buschhorn, S.T., Bauhofer, W., and Schulte, K. (2013). Comparison of new conductive adhesives based on silver and carbon nanotubes for solar cells interconnection. Sol. Energy Mater. Sol. Cells *109*, 155–159. https://doi.org/10.1016/j.solmat.2012.10.020.

22. Yüce, C., Okamoto, K., Karpowich, L., Adrian, A., and Willenbacher, N. (2019). Non-volatile free silver paste formulation for front-side metallization of silicon solar cells. Sol. Energy Mater. Sol. Cells *200*, 110040. https://doi.org/10.1016/j.solmat.2019.110040.

23. Yu, C., Zou, Q., Wang, Q., Zhao, Y., Ran, X., Dong, G., Peng, C.W., Allen, V., Cao, X., Zhou, J., et al. (2023). Silicon solar cell with undoped tin oxide transparent electrode. Nat. Energy *8*, 1119–1125. https://doi.org/10.1038/s41560-023-01331-7.

24. Weber, J., and Rößler, T. (2023). Electrically conductive adhesive-free interconnection of shingle solar cells. Sol. Energy Mater. Sol. Cells *261*, 112517. https://doi.org/10.1016/j.solmat.2023.112517.

25. Paschen, J., Baliozian, P., John, O., Lohmüller, E., Rößler, T., and Nekarda, J. (2022). FoilMet®-Interconnect: Busbarless, electrically conductive adhesive-free, and solder-free aluminum interconnection for modules with shingled solar cells. Progress in Photovoltaics. *30*, 889–898. https://doi.org/10.1002/pip.3470.

26. Oh, W., Jee, H., Bae, J., and Lee, J. (2022). Busbar-free electrode patterns of crystalline silicon solar cells for high density shingled photovoltaic module. Sol. Energy Mater. Sol. Cells *243*, 111802. https://doi.org/10.1016/j.solmat.2022.111802.

27. Solar, D. (2023). Featuring TOPCon3.0 Plus technology, DAS Solar shows up with the N-type 3.0 BBF module. https://www.das-solar.com/au/site/news_details/1193.

28. Barnett, A., Kirkpatrick, D., Honsberg, C., Moore, D., Wanlass, M., Emery, K., Schwartz, R., Carlson, D., Bowden, S., Aiken, D., et al. (2009). Very High Efficiency Solar Cell Modules. Progress in Photovoltaics. *17*, 75–83. https://doi.org/10.1002/pip.

29. Wendlandt, S. (2021). Reliability of high density "gapless" module designs. In NREL PV Reliability Workshop 2021.

30. Petter Jelle, B., Breivik, C., and Drolsum Røkenes, H. (2012). Building integrated photovoltaic products: A state-of-the-art review and future research opportunities. Sol. Energy Mater. Sol. Cells *100*, 69–96. https://doi.org/10.1016/j.solmat.2011.12.016.

31. Root, S.E., Savagatrup, S., Printz, A.D., Rodriquez, D., and Lipomi, D.J. (2017). Mechanical Properties of Organic Semiconductors for Stretchable, Highly Flexible, and Mechanically Robust Electronics. Chem. Rev. *117*, 6467–6499. https://doi.org/10.1021/acs.chemrev.7b00003.

32. Ouyang, J., and Yang, Y. (2006). Conducting polymer as transparent electric glue. Adv. Mater. *18*, 2141–2144. https://doi.org/10.1002/adma.200502475.

33. Derakhshankhah, H., Mohammad-Rezaei, R., Massoumi, B., Abbasian, M., Rezaei, A., Samadian, H., and Jaymand, M. (2020). Conducting polymer-based electrically conductive adhesive materials: design, fabrication, properties, and applications. J. Mater. Sci. Mater. Electron. *31*, 10947–10961. https://doi.org/10.1007/s10854-020-03712-0.

34. Li, N., Li, Y., Cheng, Z., Liu, Y., Dai, Y., Kang, S., Li, S., Shan, N., Wai, S., Ziaja, A., et al. (2023). Bioadhesive Polymer Semiconductors and Transistors for Intimate Biointerfaces, *693*, pp. 686–693. https://doi.org/10.1126/science.adg8758.

35. Inoue, A., Yuk, H., Lu, B., and Zhao, X. (2020). Strong adhesion of wet conducting polymers on diverse substrates. Sci. Adv. *6*. eaay5394-11. https://doi.org/10.1126/sciadv.aay5394.

36. Chen, A.X., Esparza, G.L., Simon, I., Dunfield, S.P., Qie, Y., Bunch, J.A., Blau, R., Lim, A., Zhang, H., Brew, S.E., et al. (2023). Effect of Additives on the Surface Morphology, Energetics, and Contact Resistance of PEDOT:PSS. ACS Appl. Mater. Interfaces *15*, 38143–38153. https://doi.org/10.1021/acsami.3c08341.

37. Shi, H., Liu, C., Jiang, Q., and Xu, J. (2015). Effective Approaches to Improve the Electrical Conductivity of PEDOT:PSS: A Review. Adv. Electron. Mater. *1*, 1–16. https://doi.org/10.1002/aelm.201500017.

38. Tang, H., Liang, Y., Liu, C., Hu, Z., Deng, Y., Guo, H., Yu, Z., Song, A., Zhao, H., Zhao, D., et al. (2022). A solution-processed n-type conducting polymer with ultrahigh conductivity. Nature *611*, 271–277. https://doi.org/10.1038/s41586-022-05295-8.

39. Ke, Z., Abtahi, A., Hwang, J., Chen, K., Chaudhary, J., Song, I., Perera, K., You, L.,

Baustert, K.N., Graham, K.R., et al. (2022). Highly Conductive and Solution-Processable n-Doped Transparent Organic Conductor. J. Am. Chem. Soc. *145*, 3706–3715. https://doi.org/10.1021/jacs.2c13051.

40. Nevrela, J., Micjan, M., Novota, M., Kovacova, S., Pavuk, M., Juhasz, P., Kovac, J., Jakabovic, J., and Weis, M. (2015). Secondary doping in poly(3,4-ethylenedioxythiophene):Poly(4-styrenesulfonate) thin films. J. Polym. Sci. B Polym. Phys. *53*, 1139–1146. https://doi.org/10.1002/polb.23754.

41. Nardes, A.M., Kemerink, M., de Kok, M.M., Vinken, E., Maturova, K., and Janssen, R.A.J. (2008). Conductivity, work function, and environmental stability of PEDOT:PSS thin films treated with sorbitol. Org. Electron. *9*, 727–734. https://doi.org/10.1016/j.orgel.2008.05.006.

42. Keene, S.T., Michaels, W., Melianas, A., Quill, T.J., Fuller, E.J., Giovannitti, A., McCulloch, I., Talin, A.A., Tassone, C.J., Qin, J., et al. (2022). Efficient Electronic Tunneling Governs Transport in Conducting Polymer-Insulator Blends. J. Am. Chem. Soc. *144*, 10368–10376. https://doi.org/10.1021/jacs.2c02139.

43. Akhmad, K., Kitamura, A., Yamamoto, F., Okamoto, H., Takakura, H., and Hamakawa, Y. (1997). Outdoor performance of amorphous silicon and polycrystalline silicon PV modules. Sol. Energy Mater. Sol. Cells *46*, 209–218.

44. Ghani, F., Rosengarten, G., Duke, M., and Carson, J.K. (2015). On the influence of temperature on crystalline silicon solar cell characterisation parameters. Sol. Energy *112*, 437–445. https://doi.org/10.1016/j.solener.2014.12.018.

45. Khenkin, M.V., Katz, E.A., Abate, A., Bardizza, G., Berry, J.J., Brabec, C., Brunetti, F., Bulović, V., Burlingame, Q., Di Carlo, A., et al. (2020). Consensus statement for stability assessment and reporting for perovskite photovoltaics based on ISOS procedures. Nat. Energy *5*, 35–49. https://doi.org/10.1038/s41560-019-0529-5.

46. Dupont, S.R., Novoa, F., Voroshazi, E., and Dauskardt, R.H. (2014). Decohesion kinetics of PEDOT:PSS conducting polymer films. Adv. Funct. Mater. *24*, 1325–1332. https://doi.org/10.1002/adfm.201302174.

47. Duc, C., Malliaras, G.G., Senez, V., and Vlandas, A. (2018). Long-term ageing of PEDOT:PSS: wettability Study. Synth. Met. *238*, 14–21. https://doi.org/10.1016/j.synthmet.2018.02.003.

48. Vitoratos, E., Sakkopoulos, S., Dalas, E., Paliatsas, N., Karageorgopoulos, D., Petraki, F., Kennou, S., and Choulis, S. (2009). Thermal degradation mechanisms of PEDOT:PSS. Org. Electron. *10*, 61–66. https://doi.org/10.1016/j.orgel.2008.10.008.

49. Bontapalle, S., and Varughese, S. (2020). Understanding the mechanism of ageing and a method to improve the ageing resistance of conducting PEDOT:PSS films. Polym. Degrad. Stabil. *171*, 109025. https://doi.org/10.1016/j.polymdegradstab.2019.109025.

50. Kempe, M.D., Dameron, A.A., and Reese, M.O. (2014). Evaluation of moisture ingress from the perimeter of photovoltaic modules. Progress in Photovoltaics. *22*, 1159–1171. https://doi.org/10.1002/pip.

51. Cheacharoen, R., Boyd, C.C., Burkhard, G.F., Leijtens, T., Raiford, J.A., Bush, K.A., Bent, S.F., and McGehee, M.D. (2018). Encapsulating perovskite solar cells to withstand damp heat and thermal cycling. Sustain. Energy Fuels *2*, 2398–2406. https://doi.org/10.1039/c8se00250a.

52. Stepien, L., Roch, A., Tkachov, R., Leupolt, B., Han, L., van Ngo, N., and Leyens, C. (2017). Thermal operating window for PEDOT:PSS films and its related thermoelectric properties. Synth. Met. *225*, 49–54. https://doi.org/10.1016/j.synthmet.2016.11.017.

53. Jones, C.B., Hamzavy, B., Hobbs, W.B., Libby, C., and Lavrova, O. (2018). IEC 61215 Qualification Tests vs Outdoor Performance using Module Level in Situ I-V Curve Tracing Devices. 2018 IEEE 7th World Conf. Photovolt. Energy Conversion, WCPEC 2018 - A Jt. Conf. 45th IEEE PVSC, 28th PVSEC 34th EU PVSEC, pp. 1286–1291. https://doi.org/10.1109/PVSC.2018.8548222.

54. Louwen, A., Van Sark, W., Schropp, R., and Faaij, A. (2016). A cost roadmap for silicon heterojunction solar cells. Sol. Energy Mater. Sol. Cells *147*, 295–314. https://doi.org/10.1016/j.solmat.2015.12.026.

55. Hart, P.W., and Sommerfeld, J.T. (1997). Cost Estimation of Specialty Chemicals from Laboratory-Scale Prices. Cost Eng. *39*, 31–35.

56. Davidsson, S., and Höök, M. (2017). Material requirements and availability for multi-terawatt deployment of photovoltaics. Energy Pol. *108*, 574–582. https://doi.org/10.1016/j.enpol.2017.06.028.

57. Ansanelli, G., Fiorentino, G., Tammaro, M., and Zucaro, A. (2021). A Life Cycle Assessment of a recovery process from End-of-Life Photovoltaic Panels. Appl. Energy *290*, 116727. https://doi.org/10.1016/j.apenergy.2021.116727.

58. Tune, D., Wienands, K., Ullmann, I., Devoto Acevedo, M., Timofte, T., and Halm, A. (2021). Electrically Conductive Adhesive Interconnects: How Low Can You Go. https://doi.org/10.4229/EUPVSEC20212021-4AV.1.16.

59. Söderström, T., Papet, P., and Ufheil, J. (2013). Smart wire connection technology. In 28th European Photovoltaic Solar Energy Conference and Exhibition, pp. 495–499.

60. Chen, A.X., Kleinschmidt, A.T., Choudhary, K., and Lipomi, D.J. (2020). Beyond Stretchability: Strength, Toughness, and Elastic Range in Semiconducting Polymers. Chem. Mater. *32*, 7582–7601. https://doi.org/10.1021/acs.chemmater.0c03019.

61. Namsheer, K., and Rout, C.S. (2021). Conducting polymers: a comprehensive review on recent advances in synthesis, properties and applications. RSC Adv. *11*, 5659–5697. https://doi.org/10.1039/d0ra07800j.

62. Sutjianto, J.G., Yoo, S.H., Westerman, C.R., Jackson, T.N., Wilker, J.J., and Gomez, E.D. (2023). Blends of Conjugated and Adhesive Polymers for Sticky Organic Thin-Film Transistors. Adv. Electron. Mater. *9*, 1–8. https://doi.org/10.1002/aelm.202300422.

63. Chen, A.X., Pazhankave, S.S., Bunch, J.A., Lim, A., Choudhary, K., Esparza, G.L., Runser, R., Hoover, C.G., and Lipomi, D.J. (2023). Adhesive Properties of Semiconducting Polymers: Poly(3-alkylthiophene) as an Ersatz Glue. Chem. Mater. *35*, 3329–3342. https://doi.org/10.1021/acs.chemmater.3c00485.

64. Awaja, F., Gilbert, M., Kelly, G., Fox, B., and Pigram, P.J. (2009). Adhesion of polymers. Prog. Polym. Sci. *34*, 948–968. https://doi.org/10.1016/j.progpolymsci.2009.04.007.

65. Peak, C.W., Wilker, J.J., and Schmidt, G. (2013). A review on tough and sticky hydrogels. Colloid Polym. Sci. *291*, 2031–2047. https://doi.org/10.1007/s00396-013-3021-y.

66. Blau, R., Chen, A.X., Polat, B., Becerra, L.L., Runser, R., Zamanimeymian, B., Choudhary, K., and Lipomi, D.J. (2022). Intrinsically Stretchable Block Copolymer Based on PEDOT:PSS for Improved Performance in Bioelectronic Applications. ACS Appl. Mater. Interfaces *14*, 4823–4835. https://doi.org/10.1021/acsami.1c18495.

67. Park, J., Oh, W., Park, H., Jeong, C., Choi, B., and Lee, J. (2019). Analysis of solar cells interconnected by electrically conductive adhesives for high-density photovoltaic modules. Appl. Surf. Sci. *484*, 732–739. https://doi.org/10.1016/j.apsusc.2019.03.307.